Time variations of narrow absorption lines in high resolution quasar spectra[⋆]

P. Boissé[1,2], J. Bergeron[1,2], J. X. Prochaska[3], C. Péroux[4], D. G. York[5]

[1] Sorbonne Universités, UPMC Univ. Paris 06, UMR 7095, Institut d'Astrophysique de Paris, F-75014, Paris, France
e-mail: boisse@iap.fr
[2] CNRS, UMR 7095, Institut d'Astrophysique de Paris, F-75014, Paris, France
[3] UCO/Lick Observatory, UC Santa Cruz, Santa Cruz, CA 95064, USA
[4] Aix Marseille Université, CNRS, LAM (Laboratoire dAstrophysique de Marseille) UMR 7326, F-13388 Marseille, France
[5] Department of Astronomy, University of Chicago, 5640 South Ellis Avenue, Chicago, IL 60637, USA

ABSTRACT

Aims. We have searched for temporal variations of narrow absorption lines in high resolution quasar spectra. A sample of five distant sources have been assembled, for which two spectra - either VLT/UVES or Keck/HIRES - taken several years apart are available.
Methods. We first investigate under which conditions variations in absorption line profiles can be detected reliably from high resolution spectra, and discuss the implications of changes in terms of small-scale structure within the intervening gas or intrinsic origin. The targets selected allow us to investigate the time behavior of a broad variety of absorption line systems, sampling diverse environments: the vicinity of active nuclei, galaxy halos, molecular-rich galaxy disks associated with damped Lyα systems, as well as neutral gas within our own Galaxy.
Results. Intervening absorption lines from Mg II, Fe II or proxy species with lines of lower opacity tracing the same kind of (moderately ionised) gas appear in general to be remarkably stable (1σ upper limits as low as 10% for some components on scales in the range 10 - 100 au), even for systems at $z_{abs} \approx z_e$. Marginal variations are observed for Mg II lines toward PKS 1229−021 at $z_{abs} = 0.83032$; however, we detect no systems displaying changes as large as those reported in low resolution SDSS spectra. The lack of clear variations for low β Mg II systems does not support the existence of a specific population of absorbers made of swept up gas toward blazars. In neutral or diffuse molecular media, clear changes are seen for Galactic Na I lines toward PKS 1229−02 (decrease of N by a factor of four for one of the five components over 9.7 yr), corresponding to structure at a scale of about 35 au, in good agreement with known properties of the Galactic interstellar medium. Tentative variations are detected for H$_2$ $J = 3$ lines toward FBQS J2340−0053 at $z_{abs} = 2.05454$ ($\simeq 35$% change in column density, N, over 0.7 yr in the rest-frame), suggesting the existence of structure at the 10 au-scale for this warm molecular gas. A marginal change is also seen in C I from another velocity component of the same absorption system ($\simeq 70$% variation in N(C I).

Key words. Quasars: absorption lines – ISM: structure

1. Introduction

Absorption lines in distant active galactic nuclei (AGN) spectra have long been recognized as an invaluable source of information on diffuse material lying all along these lines of sight (LoS), from local interstellar material within the Milky Way, disks or halos of intervening galaxies, intergalactic clouds, up to gas located in the vicinity of the AGN itself. As illustrated by numerous studies (see e.g. Noterdaeme et al. 2007; Neeleman et al. 2015) many properties of the gas can be investigated through a detailed analysis of the absorption lines, including ionization level, chemical composition, density and temperature.

Aside from the broad absorption lines (BAL) and intrinsic narrow absorption lines which often display time variations over timescales of months or years in the absorber's frame (Hamann et al. 2008, 2011; Filiz Ak et al. 2013 and references therein; Misawa et al. 2014; Grier et al. 2015) intervening absorption systems observed in quasar spectra are thought to be essentially

stable in time. However, a recent study based on multi-epoch low resolution SDSS spectra (Hacker et al. 2013) suggests that some narrow intervening systems (mainly Mg II and Fe II) might also display variability. These authors propose that time changes are due to the transverse motion of the LoS through the absorber coupled to the presence of structure in the absorbing gas at scales in the range 10 - 100 au, similar to that observed for diffuse neutral gas in our own Galaxy (Crawford 2003; Lauroesch 2007, Welty 2007, Meyer et al. 2012). Indeed, transverse peculiar velocity values of a few 100 km s^{-1} are expected for the target, the observer and the intervening gas, which imply drifts over a few years falling in this range (recall that 1 au yr^{-1} is equivalent to 4.67 km s^{-1}).

Information on spatial structure within the low-ionization medium similar to the one probed by multi-epoch SDSS spectra remains quite limited. Observations of gravitationally lensed quasars with multiple images have been used to investigate spatial variations over scales of a few 100 pc. In particular, Rauch et al. (2002) studied the behavior of Mg II - Fe II systems along three adjacent LoS toward Q2237+0305 and by comparing the line profiles, infer a lower limit of about 0.5 kpc for the overall absorber extent and a typical size of the order of

---

100 pc for cloudlets associated with individual velocity components. Similarly, toward the lensed QSO pair APM 08279+5255, Kobayashi et al. (2002) derived an estimate for the cloudlet size of 200 pc, in good agreement with values inferred from modelling of these absorbers (Churchill & Charlton 1999; Crighton et al. 2015). Such observations are restricted to a few systems and do not enable a study of the structure at smaller scales. In our own Galaxy, structure in the low-ionization medium has been investigated by Welty (2007) who found no change in O I, Si II, S II and Fe II lines over tens of au. Thus, the limited information available (see also the recent study by Neeleman et al. 2015) does not suggest the presence of significant structure over scales as small as 100 au in the low-ionization medium, comparable to the one seen in the neutral medium.

The results obtained by Hacker et al. (2013) then appear somewhat puzzling and require additional investigations. Their study is based on low resolution SDSS spectra which can only provide equivalent width measurements and do not give access to the true line profiles and to the identification of the individual absorption velocity components. If some absorption lines do vary, changes most probably affect only some velocity components and should be much more apparent in high resolution spectra. High resolution line profiles would also be very useful to assess the reality of any variation detection. Indeed, when spectral profiles are resolved (or at least partially resolved), changes in a specific transition from a given species imply a corresponding change for other transitions from the same species that can be computed a priori, providing a stringent reliability test. Furthermore, high resolution data will minimize the impact of various artefacts like imperfect sky subtraction, bad pixels etc.

Good signal-to-noise (S/N) high resolution quasar spectra have been taken routinely over the last 15 years (for instance, in the context of Large Programs conducted on 8 - 10m class telescopes; see e. g. Bergeron et al. 2004 and Molaro et al. 2013) and for some distant sources, several observations have been performed over time intervals reaching ten years. We have thus gathered a sample of five sources with at least two VLT/UVES or Keck/HIRES spectra taken several years apart. In one case, we acquired a spectrum specifically for this study. These lines of sight altogether include a broad variety of systems, probing various environments ranging from neutral Galactic gas, galaxy disks at intermediate redshifts (i.e. damped Lyα system), Mg II-Fe II systems due to intervening galaxy halos as well as systems with a redshift close to the emission redshift. Several of our targets fall in the blazar category, which will allow us to investigate the possible presence of narrow systems with a large ejection velocity, in line with the scenario put forward by Bergeron et al. (2011).

The purpose of our study is to explore the potential of multi-epoch high-resolution observations of AGN to investigate the small-scale structure in intervening gas and possible intrinsic variations for narrow low ejection velocity systems. In Sect. 2, we describe the method (expected LoS drifts, selection of transitions which are best suited for a search of variations, etc) while the data and raw results are presented in Sect. 3. Their implications are discussed in Sect. 4. We summarize our results and mention some prospects for further variability studies in Sect. 5.

2. Detecting absorption line variations

When considering two spectra of the same target taken over some time interval, an important parameter is the drift of the LoS relative to a foreground absorber. We shall first discuss how one can estimate this scalelength over which the comparison of the

two observations will provide structure information. Next, we examine which line parameters (the opacity in particular) yield the best sensitivity to a given fractional column density change. Finally, we discuss methods which can be used to reliably detect line variations and assess their significance.

2.1. Line of sight drifts relative to the absorber

For now, we consider that the target is point-like and defines an "ideal" LoS, intersecting an intermediate redshift absorber at point M (hereafter the "impact point"; Fig. 1). As mentioned above, it is the combination of small-scale density or velocity structure in the intervening gas and the transverse motion of the LoS through this material which can potentially induce line variations. The appropriate frame for computing the velocities of interest is a cosmological one, in which the Cosmic Microwave Background (CMB) is globally isotropic. The motion of both the target and the observer determines the drift of the LoS in this frame. The observer's motion is due mainly to the peculiar motion of the Milky Way and to Galactic rotation. The combination of the two corresponding velocities is directly constrained by the detection of the dipolar anisotropy in the CMB radiation indicating that the Solar System is moving at 368 ± 2 km s^{-1} relative to the observable Universe toward the direction $l_o = 263.85$ deg and $b_o = 48.25$ deg (Fixsen et al. 1996).

Let us denote by $\mathbf{V_O}$ the corresponding velocity vector. Consider a target T with Galactic coordinates (l_T, b_T) and let $\mathbf{u_T}$ be the unit vector pointing in this direction (Fig. 1). We are concerned only by the transverse component, thus by the projection, $\mathbf{V_{O\perp}}$, of $\mathbf{V_O}$ onto a plane normal to $\mathbf{u_T}$. This projected velocity can be written as

$$\mathbf{V_{O\perp}} = \mathbf{V_O} - (\mathbf{u_T} . \mathbf{V_O}) \mathbf{u_T} = V_O (\mathbf{u_O} - (\mathbf{u_T} . \mathbf{u_O}) \mathbf{u_T}), \tag{1}$$

where $\mathbf{V_O} = V_O . \mathbf{u_O}$. From these relations, and using the components $(\cos b_T \cos l_T, \cos b_T \sin l_T, \sin b_T)$ of the unit vector associated with Galactic coordinates (l_T, b_T), it is straightforward to compute $V_{O,\perp}$ for any specific target (for the five targets listed in Table 1, $V_{O,\perp} = 288, 368, 129, 365$ and 12 km s^{-1} respectively). In the most favorable case for which $V_{O,\perp} = V_O$, this motion alone results in a shift of about 4×10^{-3} pc or 800 au near the observer, over a time interval of 10 years.

Unfortunately, we cannot estimate the transverse velocity of the target because the proper motion onto the sky is much too small to be measurable, contrary to interstellar medium studies, in which the proper motion of nearby bright stars is known. Unless the target belongs to a peculiar environment like a galaxy cluster or experienced an ejection event, the magnitude of its peculiar velocity should be also of the order of a few 100 km s^{-1}. The transverse velocity of the impact point M, can then be written as,

$$\mathbf{V_{M\perp}} = \alpha \, \mathbf{V_{T\perp}} + (1 - \alpha) \, \mathbf{V_{O\perp}}, \tag{2}$$

where $\alpha = d_A/d_T$, d_A being the distance to the absorber and d_T that to the target. Finally, one must take into account the velocity $\mathbf{V_A}$ of the absorber in the cosmological frame or rather its transverse component, $\mathbf{V_{A\perp}}$. In the end, the value of interest is the relative drift velocity

$$\mathbf{V_d} = \mathbf{V_{M\perp}} - \mathbf{V_{A\perp}}. \tag{3}$$

Again, $\mathbf{V_{A\perp}}$ cannot be determined (interstellar studies suffer from the same difficulty) and only a typical value of a few hundreds of km s^{-1} can be considered (as with the observer,
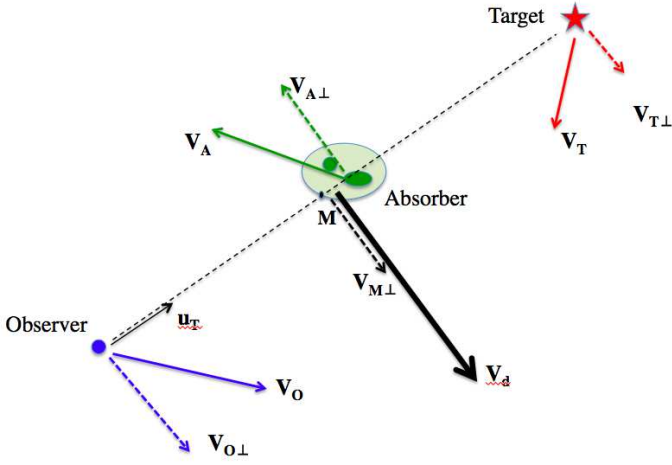
Fig. 1. The observer and target move with 3D velocities $\mathbf{V_O}$ and $\mathbf{V_T}$ in the cosmological frame. Their transverse component $\mathbf{V_{O\perp}}$ and $\mathbf{V_{T\perp}}$ determines the transverse velocity $\mathbf{V_{M\perp}}$ of the impact point M. The latter combines with the transverse velocity of the absorber $\mathbf{V_{A\perp}}$ to define the relative drift velocity of the LoS with respect to the gas, $\mathbf{V_d}$, which sets the scale probed within the absorber during a given time interval.

the actual value results from the combination of the bulk intervening galaxy motion and of the absorbing gas internal kinematics, e.g. rotation, infall or outflow). A maximum value for the drift velocity, V_d, can be estimated assuming an optimal configuration in which $\mathbf{V_{O\perp}}$ and $\mathbf{V_{T\perp}}$ are parallel while $\mathbf{V_{A\perp}}$ points in the opposite direction. In that case, V_d can reach values $V_d = \max(V_{O\perp}, V_{T\perp}) + V_{A\perp}$, as large as about 500 km s^{-1}.

Eqs. (2) and (3) are valid in the local 3D space. On large cosmological scales, there is no unique way to define distances. Thus, these relations can hold only at low redshifts where all cosmological distances become equivalent. Since the exact values of both $V_{T\perp}$ and $V_{A\perp}$ are unknown for any specific target, it is sufficient for our purpose to estimate drift velocities by i) inserting into the above equations typical values for $V_{T\perp}$ and $V_{A\perp}$, ii) using the angular size distance for d, and iii) taking into account time dilation (a time interval Δt in the observer's frame corresponds to $\Delta t/(1 + z_A)$ or $\Delta t/(1 + z_T)$ in the absorber's or target's frame respectively, which is equivalent to reduce $V_{A\perp}$ and $V_{T\perp}$ by a factor of $(1 + z_A)$ or $(1 + z_T)$).

In fact, a quasar is an extended continuum source with a typical size in the range 10 - 100 au (the size of the accretion disk responsible for the optical emission; Dai et al. 2010). Thus, contrary to observations of moving stars used to probe interstellar gas structure, significant averaging of the foreground structure can occur, implying a reduced amplitude for absorption line variations. The situation may be different for blazars. These sources undergo spectacular photometric variations and, when in a "high state", their continuum is dominated by emission from the relativistic jet. Changes in the morphology of the source itself can also occur, which would be equivalent to an additional contribution to the drift of the LoS. Time changes in the 21 cm absorption seen toward AO 0235+164 and PKS 1127−14 by Wolfe et al (1982) and Kanekar & Chengalur (2001) are precisely attributed to such an effect.

When dealing with absorption by Galactic interstellar material (four out of our five selected targets display relatively strong Ca II or Na I absorption from Milky Way gas), the appropriate frame to consider is the Local Standard of Rest (LSR) in which

interstellar gas is at rest in average. In this case, the drift of the LoS is determined by the peculiar motion of the Sun in this frame, $\mathbf{V_S}$, or more specifically, by its projection onto a plane perpendicular to the LoS considered. This question is discussed in more detail in Boissé et al. (2013).

2.2. Sensitivity to absorption line variations

In order to select the absorption lines which are best suited to search for time variations, we now quantify the sensitivity to a given fractional column density (N) change. Obviously, very weak or, on the contrary, saturated features will be of little use: there must be some optimal intermediate value for the opacity.

Consider a fully resolved normalised profile, $I_n(v)$, expressed in the velocity scale,

$$I_n(v) = e^{-\tau(v)}, \qquad (4)$$

where $\tau(v)$ is the line opacity at velocity v, written as

$$\tau(v) = k\,\lambda_0\,f\,N(v), \qquad (5)$$

where k is a constant, λ_0 the rest wavelength of the transition, f the oscillator strength and $N(v)\,dv$ the column density for species within the velocity interval $[v, v + dv]$. Let us first assume a spectrum noise which is independent on I_n. The sensitivity can then be expressed as

$$\left| \frac{\delta I_n}{\delta N/N} \right| = \tau\,e^{-\tau}. \qquad (6)$$

It reaches its maximum at $\tau = 1$ for which $I_n \approx 0.37$. The interval over which the sensitivity is reduced by less than 20% is $0.61 \leq \tau \leq 1.53$, which corresponds to $0.22 \leq I_n \leq 0.54$.

An alternative case of interest is that of photon noise, for which the spectrum r.m.s. follows a $\sqrt{I_n}$ law; the ability to detect a given variation δI_n is then proportional to

$$\left| \frac{\delta I_n}{\sqrt{I_n}\,\delta N/N} \right| = \tau\,e^{-\frac{\tau}{2}}. \qquad (7)$$

This expression reaches its maximum at $\tau = 2$ where $I_n \approx 0.14$ (the sensitivity remains good in the sense defined above for $1.2 \leq \tau \leq 3.1$). In practise, observed spectra are within these two extreme cases; we conclude that the sensitivity for the detection of variations is optimal for *intermediate* opacity values (typically 1.5), corresponding to normalised intensities of about 0.2.

One should keep in mind that generally, depending on the instrumental resolution and Doppler b parameter value, absorption profiles will not be fully resolved, implying apparent opacities lower than the true ones (Savage & Sembach 1991). For instance, with an instrumental resolution of 6.6 km s^{-1}, the depth of a Gaussian line is reduced by a factor of 0.45 for $b = 2$ km s^{-1}. Then, if the true opacity at line center is $\tau_0 = 1$, the apparent opacity becomes 0.33. Therefore, to conclude on the sensitivity of a given line to changes in N, one cannot rely only on its observed profile. Fortunately, several transitions from the same species are often available with various f values. Simultaneous fitting of the corresponding line profiles will then allow us to determine the true opacity and assess whether or not these transitions are appropriate for a variability search.

2.3. Characterisation of line variations

Our aim is to detect line profile variations and to quantify their significance. A first direct indication can be obtained by superposing the two successive spectra after careful normalisation and adjustment of the wavelength scales if necessary. Such a raw comparison is meaningful only if the spectral resolution, R, is the same at the two epochs. If this is not the case, the higher R spectrum has to be degraded to the lower resolution value. Fortunately, the HIRES and UVES data used in this paper have very similar nominal resolutions - FWHM = 6.25 and 6.6 km s^{-1} respectively - and we could verify that, given the S/N ratio, such a slight difference has a negligible effect on the profile of the absorption features discussed in this paper (cf Sect. 3). Differences in the line spread function (LSF) might also play a role. One can use unresolved lines to check that such an effect does not affect the comparison of successive profiles.

It turns out that for the systems investigated here, the two successive spectra available rarely display marked, unambiguously significant differences. Thus, in order to i) increase our ability to detect weak variations by relying on the presence of several transitions from a given species (e.g. Fe II, or H$_2$) and ii) take into account differing R values if necessary, a more powerful method is to simultaneously fit all profiles corresponding to these transitions, at each epoch. To this purpose, we used VPFIT[1] a routine which uses multicomponent Voigt profiles (convolved with the instrument profile, which we assume to be Gaussian here) and yields the redshift z_i, column density N_i and Doppler parameter b_i for each velocity component, together with their 1σ uncertainties. Comparison of the values obtained for each epoch then allows us to determine whether some of these parameters have undergone significant time changes. In all cases, the same sets of components were appropriate to fit the profiles at both epochs, with no significant change in z_i, nor in b_i. Some time variations in N_i are detected or suspected for a few absorptions systems (see Sect. 3). To assess their significance, we compute the difference between epoch 1 and 2, $\Delta N_i = N_{i,2} - N_{i,1}$ and its uncertainty $\sigma(\Delta N_i)$ by combining uncertainties on $N_{i,1}$ and $N_{i,2}$ in quadrature. This procedure provides a formal significance which properly takes into account the noise level in both spectra. Other sources of uncertainty related to continuum placement or to the choice of velocity components are more difficult to quantify, especially when variations are small. As a conservative approach, variations with a significance level above 3.5σ and an associated relative column density variation, $\Delta N/\langle N \rangle$ above 25% are qualified as "significant". Variations at more than 2σ but which do not fulfill these two criteria are considered as marginal.

When several transitions from the same species are available, the quality of the fit obtained provides a stringent test of the internal consistency of the data and gives a powerful means to rule out false variations due to instrumental artefacts. Indeed, changes must not only be present for all transitions but their magnitude must be consistent with the f values. In this regard, species such as Fe II, C I, or H$_2$, which display many transitions from a given level within a relatively narrow wavelength interval are especially suitable to probe weakly ionized, neutral or molecular gas, respectively.

Often, several species can be used to trace a given phase (e.g. Mg II, Fe II, S II for weakly ionized gas). One can then select among all lines detected from these species those i) which opacity falls in the optimal range discussed above, and ii) occurring in spectral regions of good S/N ratio.

---

[1] http://www.ast.cam.ac.uk/ rfc/vpfit.html

3. Variability study of five blazars with low-moderate β systems

3.1. The absorber sample

One of our initial motivations was to explore the link between gas swept by the AGN jet and low β absorbers, as suggested by Bergeron et al. (2011). We then investigated among their blazar sample objects with jets, thus radio-loud and γ-ray emitters (detected by Egret, Integral or Fermi/LAT). An additional selection criterion is the existence of Mg II absorption systems at low relative velocity $\beta \equiv \Delta v(z_{\rm em}, z_{abs})/c < 0.15$ with a rest-frame equivalent width $W_r(2796) > 0.3$ Å, as well as intervening systems and Damped Ly-α (DLA) systems at high β. We then searched the VLT-UVES and Keck-HIRES archives for high-spectral resolution spectra of this blazar subsample, and selected targets observed several years apart, possibly about one decade. We checked that the signal-to-noise per pixel was S/N $\gtrsim 10$ for the main absorptions of interest: the Mg II doublets at $\beta < 0.15$ and the Galactic Na I doublets.

One blazar satisfying the above selection criteria, is the extensively studied, highly variable BL Lac object AO 0235+164 for which variations of 21 cm intervening absorption at $z_{\rm abs} = 0.524$ had been reported three decades ago (Wolfe et al. 1982). This absorber has been identified as a BAL quasar with very faint extended emission (Burbidge et al. 1996). The variations were interpreted as most probably due to variations in the brightness distribution of the background radio source. Another blazar is PKS 1741−038, which was re-observed by us with UVES in 2011 to search for variability of its two strong Mg II absorbers at $\beta = 0.074$ and 0.287. For both objects, the available UVES and HIRES spectra have been obtained at epochs about 9.5 yr apart in the observer's frame.

We also searched for high resolution spectra of PKS 1229−02, a blazar for which we obtained deep HST imaging showing optical emission associated with knots in the radio jet (Le Brun et al. 1997). There is a DLA system at $z_{\rm abs} = 0.3950$ with associated 21 cm absorption, and several Mg II absorbers at $\beta \leq 0.15$. The above selection criteria are also met for this source and there are two sets of high S/N UVES spectra taken at epochs 9.2 yr apart.

Finally, there are HIRES and UVES data available for two targets with C I absorption at $z_{\rm abs} \sim 1.5$ with associated 21 cm absorption at high β (Kanekar et al. 2010): PKS 0458−020 ($z_{\rm abs} = 1.5606$) and FBQS J2340−0053 ($z_{\rm abs} = 1.3608$), the latter with observations about two years apart. In the radio spectrum of PKS 0458−020, variable 21 cm absorption on timescale of months has been detected at $z_{\rm abs} = 2.0395$ (Kanekar et al. 2014 and references therein). There are also DLA systems at low $\beta \leq 0.10$ toward PKS 0458−020 at $z_{\rm abs} = 2.0395$ and FBQS J2340−0053 at $z_{\rm abs} = 2.0545$. The physical conditions in the low β DLA system of FBQS J2340−0053, with associated C I absorption, have been investigated by Jorgenson et al. (2010). The multiple system at $z_{\rm abs} = 1.3608$ toward FBQS J2340−0053 has been extensively studied by Rahmani et al. (2012) to constrain the variation of fundamental constants.

Information on the sample and the observations is given in Table 1 and that on the absorption systems in Table 2. For some UVES data, we used the reduced data sets produced internally at ESO, based on the latest calibration pipelines and the best available calibration data. For the other UVES observations, the spectra were reduced by us or made available to us by several colleagues (see the acknowledgements). For HIRES spectra, the

Table 1. The sample.

target common name	class	coordinates J2000	z_{em}	spectrograph	date	λ range nm	$\Delta t, n$ min
AO 0235+164 [H]	BL-γ	023838.9+163659	0.937	HIRES	12-1997	367-612	40,4
				UVES	02-2007	303-388+58-668	60,4
PKS 0458−020	FS-γ	050112.8−015914	2.286	HIRES	02-1995	394-629	480[a]
				UVES	10-2004	390-665+670-850	75,4
PKS 1229−02	FS-γ	123200.0−022404	1.044	UVES	02-2002	326-445+458-668	60,3
				UVES	04-2011	326-445+458-668	50,1
PKS 1741−038	FS-γ	174358.8−035004	1.054	UVES	06-2001	414-621	40,2
				UVES	04-2011	414-621	50,5
FBQS J2340−0053	FS	234023.7−005327	2.085	HIRES	08-2006	306-589	250[a]
				UVES	10-2008	330-450+478-681	75,6

class - BL: BL Lac object, FS: Flat Spectrum Radio QSO (FSRQ), γ: Gamma-ray emitter. The four γ-ray emitters are blazars.
spectrograph - spectral resolution: FWHM(HIRES)=6.25 km s^{-1}, FWHM(UVES)=6.6 km s^{-1}.
$\Delta t, n$ Exposure time per individual exposure and number of exposures.
[H] In a very high state at both epochs. The new z_{em} is derived from [Ne IV] emission.
[a] Total exposure time.

data sets were reduced by Prochaska's team. All redshifts and velocities considered in the following are vacuum heliocentric.

In the analysis presented below, we estimate the variation of N between the two epochs and use the combined quadratic errors to evaluate its significance level, as described in Sect. 2.3. In case of no variation, we give the 1σ limit on $\Delta N/\langle N \rangle$, restricting this evaluation to fairly good S/N, thus meaningful limits: $\Delta N/\langle N \rangle < 50\%$.

3.2. Tracers of the Interstellar Medium

The main tracers of the local Interstellar Medium (ISM) detectable in our spectra are the Na I and Ca II doublets, Ca Iλ4227 as well as the CH$^+$$\lambda$4232 and CH$\lambda$4300 molecular lines. Diffuse interstellar bands (DIBs), mainly at 4428, 5780 and 5797 Å, could also be identified in some UVES spectra.

Toward AO 0235+164, the Galactic Na I absorption shows a strong, single component at $z_{abs} = +0.00002$. A simultaneous fit to both members of the Na I doublet yields identical values at the two epochs, 9.2 yr apart, within the 1σ errors: $N(\text{Na I}) = (2.51 \pm 0.04) \times 10^{12}$ cm^{-2}.

The Galactic Na I absorption toward PKS 1229−02 is multiple (5 components) and extends over 76 km s^{-1}. Significant variation is present for the component at $z_{abs} = -0.000127$: in 9.7 yr, it has nearly disappeared, with $N(\text{Na I})$ decreasing by a factor of four (see Table 3 and Fig. 2). The other three strong components ($N(\text{Na I}) > 10^{11}$ cm^{-2}) did not vary (1σ: 17%).

Toward PKS 1741−038, Galactic molecular absorptions at $v_{LSR} = 2$ km s^{-1} have been extensively investigated, with detections of HCO$^+$ (Lucas & Liszt 1996), CO (Akeson & Blitz 1999) and C$_2$H (Lucas & Liszt 2000), together with variable 21 cm absorption (Lazio et al. 2001). The associated Na I absorption at $z_{abs} = -0.00033$ is multiple (4 components), partly saturated and blended with atmospheric Na I emission, thus preventing a search for variations. Two well-known DIBs are detected at both epochs, at 5780 and 5797 Å. Their equivalent widths are equal to 0.33 and 0.10 Å respectively, and are similar at two epochs 9.8 yr apart, with $\Delta W/\langle W \rangle = 21\% \pm 13\%$ and 20% ±23%. Two other DIBs at 4428 and 6196 Å, the Ca II doublet and CH$^+$$\lambda$4232 are detected but are far too noisy in the 2001 spectrum to investigate variability.

Finally, toward FBQS J2340−0053, the Na I 5897 line is not covered in the HIRES spectrum. The single component of the Ca II doublet at $z_{abs} = -0.00002$ remains stable (1σ: 3.8%) within 1.9 yr.

3.3. Neutral and molecular gas at high z

Toward PKS 0458−020, C I is well detected at $z_{abs} = 1.5605$ in the HIRES spectrum (with a single component, as reported in Kanekar et al. 2010) but of too low S/N in the UVES spectrum to get useful variability constraints. In FBQS J2340−0053 spectra, C I is detected at $z_{abs} = 1.3606$ and 2.0545. The three well separated components of the lower z system are stable (1σ: 12%). The fit of C I at $z_{abs} = 2.0545$ involves a minimum of eight components, two sets being heavily blended (components 3-4 and 5-6 respectively). Within the blend at $z_{abs} = 2.05473$ a very narrow component (number 6) shows a possible variation $\Delta N/\langle N \rangle$ of 69% in 0.71 yr (rest-frame) at the 3.0σ significance level (see Table 3 and Fig. 3 left panel); the 1σ limits for the other seven components are in the range 9-50%.

Molecular hydrogen has already been detected toward FBQS J2340−0053 at $z_{abs} = 2.0545$ (Jorgenson et al. 2010). The Lyman and Werner transitions display six components (which roughly correspond to C I components number 1, 2, 3-4, 5-6, 7 and 8) and there is a possible variation of the sixth H$_2$, $J = 3$ weak component at $z_{abs} = 2.05513$. Using the unblended components of the transitions at 1081, 1084 and 1099 Å we find a decrease, $\Delta N/\langle N \rangle = -34\%$, in only 0.71 yr (rest-frame), significant at the 3.1σ level (Table 3 and Fig. 3, right panel). Unfortunately, the corresponding C I features are too weak to check whether C I lines display similar variations (note in the left panel of Fig. 3 that features at $v \simeq 40$ km s^{-1} for the C Iλ1277 and C Iλ1328 transitions are in fact dominated by C I* transitions from the strongest components). Conversely, the fourth H$_2$ component which corresponds to the second C I blend (components number 5 and 6) with marginal variations is opaque in the available transitions and thus, insensitive to time changes.

Table 2. The absorption systems.

target	z_{abs}	β	main doublet	strength	S/N[a]	associated low ions present in the 2 spectra
AO 0235+164	+0.00002		Na I	w	67 - 56	none
	0.52432	0.235	Mg II	VSm	28 - 14[b]	Mg I, Fe II, Mn II, Ca II, Ti II
	0.85142	0.045	Mg II	w	62 - 50	none
	0.85237	0.045	Mg II	S	62 - 50	Mg I, Fe II
	0.85562	0.043	Mg II	w	62 - 50	none
PKS 0458−020	0.89025	0.503	Mg II	S	11 - 13	Fe II
	1.52712	0.257	Mg II	VSm	15[b] - 5	Fe II
	1.56055	0.244	Mg II	S	14[b] - 5	C I, Fe II, Zn II, Cr II, Ni II
	2.03956	0.078	Mg II	S	10[b'] - 5	Fe II, Zn II, Cr II, Ni II, Si II
PKS 1229−02	−0.00016		Na I	w	52 - 15	Ca II
	0.39458	0.364	Mg II	VSm	44 - 13	Mg I, Fe II, Mn II, Ca II, Ti II
	0.69990	0.182	Mg II	Vw	50 - 13	none
	0.75643	0.150	Mg II	ws	50 - 13	Mg I, Fe II
	0.76836	0.144	Mg II	w	50 - 14	none
	0.83032	0.110	Mg II	w	53 - 14	Fe II
	0.83102	0.110	Mg II	Vw	53 - 14	none
	0.83128	0.109	Mg II	w	53 - 14	Fe II
PKS 1741−038	−0.00070		Na I	w	12 - 32	none
	−0.00033		Na I	S	12 - 32	DIBs
	0.52739	0.288	Mg II	w	5 - 13	none
	0.52822	0.287	Mg II	S	5 - 13	Mg I, Fe II
	0.67846	0.199	Mg II	w	8 - 18	none
	0.90799	0.074	Mg II	VSm	10 - 28	Mg I, Fe II
FBQS J2340−0053	−0.00002		Na I	S	29 - 68	Ca II
	1.36064	0.261	Mg II	VSm	30[b] - 64	C I, Fe II, Zn II, Cr II, Si II, Ni II
	2.05454	0.010	Fe II	VSm	34[b'] - 56[b']	C I, C I*, Fe II, S II, Si II

[a] : S/N per pixel around the main absorption for the older and recent epoch, respectively.
[b,b'] : Mg II region not covered; we list instead the S/N around Fe II2374-2382, Fe II1608-1611.
VSm : very strong, highly multiple absorption, $w_r(2796) \gtrsim 2.0$ Å.
S : strong absorption, $w_r(2796$ or $5891) > 0.3$ Å.
w : weak absorption, $0.02 < w_r(2796$ or $5891) < 0.3$Å.
ws : although weak, the Mg II doublet is saturated.
Vw : very weak absorption, $w_r(2796) < 0.02$ Å.

3.4. The Mg II-Fe II systems

3.4.1. Low β Mg II systems

There are only two blazars with low β Mg II systems of moderate strength. For the other three, these systems are either DLAs or extremely strong saturated Mg II absorbers; we have then searched for proxies of intermediate opacity (e.g. Fe II lines) to constrain variability.

Toward AO 0235+164, there are three Mg II systems at low β: z_{abs} = 0.8514 (three fitted components), 0.8523 (seven components) and 0.85562 (single). There is no variation of the triple and single systems (1σ limits on $\Delta N/\langle N \rangle$ of 9.5% and 6.3%, respectively). For the multiple system, one Mg II component at z_{abs} = 0.85236, blended with two weaker ones at z_{abs} = 0.85231 and 0.85241, shows a tentative variability of its column density $\Delta N/\langle N \rangle$ of 53% in 5.0 yr (absorber rest-frame), but at a low significance level of only 2.3σ (see Table 3 and Fig. 4). For these three components, the associated Fe II doublet is stable (1σ: 5.2%)

Toward PKS 1229−02, there is a triple, unblended system at z_{abs} = 0.830. The strongest component at z_{abs} = 0.83032 shows a marginal small variation $\Delta N/\langle N \rangle$ of 17% in 5.0 yr (rest-frame) at a 3.7σ significance level (Table 3 and Fig. 5). There is no variation of the associated four strongest Fe II lines (1σ: 7.3%). The systems at z_{abs} = 0.83102 and 0.83128 are too weak to derive

meaningful limits on their variabilty. There are two other Mg II systems at $\beta \leq 0.15$, and they are stable: the weak, single component doublet at z_{abs} = 0.7684 (1σ: 8.7%) and the triple system at z_{abs} = 0.7564 with one nearly saturated component (1σ: 20%).

Only one of the three targets with extremely strong saturated, low β Mg II systems has proxy lines yielding meaningful limits. Toward PKS 0458−020, the Ni II triplet and the Zn II-Cr II lines at z_{abs} = 2.03956 are all of moderate strength and heavily blended without clear variation. In PKS 1741−038 spectra, the Fe II lines are saturated. Thus, some variability constraint can only be placed on the z_{abs} = 2.0545 DLA absorber toward FBQS J2340−0053: the three strongest S II components of medium strength at z_{abs} = 2.0546 and the strongest one of Al III at z_{abs} = 2.05511 do not show variability (1σ: 32% and 28%, respectively; see Sect. 4.2).

3.4.2. High β Mg II systems

For the high β systems, variations are not detected from either their Mg II doublets or proxy lines. Toward AO 0235+164, the two strongest components of the Ca II doublet at z_{abs} = 0.5239, associated with the DLA, do not vary (1σ: 26%). Toward PKS 0458−020, the Fe II$\lambda\lambda$2344,2382 lines at z_{abs} = 1.5271 (selecting the 3 unblended components) do not vary either (1σ: 15%). Finally, toward FBQS J2340−0053, the highly multiple Fe II sys-
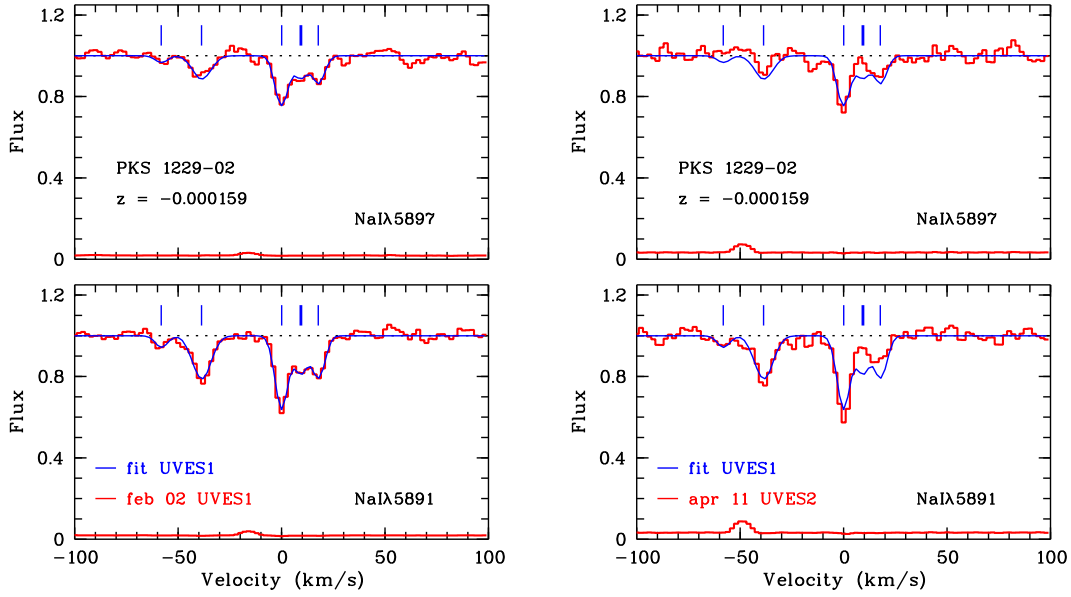
Fig. 2. Galactic Na I absorption toward PKS 1229−02: spectrum, its error (red curves) and simultaneous fit to both transitions (blue curve). The UVES 2002 data are shown in the left panel; in the right panel we display the UVES 2011 data together with the fits to the 2002 data (blue). Note the disappearance of the component at $v_{helio} = 9.6$ km s^{-1} (thick vertical tick mark), within a period of 9.2 yr. The heliocentric redshift $z = −0.000159$ (strongest component) corresponds to $v = 0$ km s^{-1}.

tem at z_{abs} = 1.3606, associated with C I and 21 cm absorptions, is stable (1σ: 14% for all the components, using the weak Fe II$\lambda\lambda$2249,2260 doublet to constrain the other nearly saturated lines).

4. Discussion

4.1. Presence of intrinsic systems in blazar spectra ?

Time variability of narrow absorption lines at low β have been securely detected in small samples of high ionization systems (involving C IV, N V and O VI), observed at low and intermediate resolution (Narayanan et al. 2004; Wise et al. 2004, Hamann et al. 2011). The lines showing variations are essentially from mini-BALs and associated (Δv < 5000 km s^{-1}) narrow-line systems. The time-scales invested (in the quasar rest-frame) range from 0.28 to 8.8 yr, and the variable narrow lines remained fixed in velocity. High and low ionization systems (at β > 0.01) with repeated observations have been identified by Hacker et al. (2013) in a very large sample of SDSS-DR7 quasar spectra: 33 out of 1084 systems have absorption lines with variations in their equivalent widths. For most of them W_r > 0.3 Å and $\Delta W_r / W_r$ > 50%, with two-thirds of the variable systems being at 'relatively low' β (< 0.22). Low ionization species are present in all the 33 variable systems and C IV is detected in the 17 systems at sufficiently high z_{abs} (> 1.50). Chen et al. (2013) focussed their variability study on associated (β < 0.03) Mg II systems identified in SDSS-DR7 and SDSS-DR9 (BOSS survey) spectra. They do not detect time variations at a significance level larger than 3σ in their sample of 36 Mg II doublets.

No variation of intervening Mg II systems in high spectral resolution spectra has been reported so far. Among the five targets in our sample, three blazars have in total six Mg II doublets at $\beta \leq 0.15$ which are suitable (unsaturated, not heavily blended lines) for variability studies. As described in Sect. 3.4, only marginal column density variations have been detected

for two z_{abs} ~ 0.85 Mg II absorbers at a significance level of 2.3σ and 3.7σ, respectively. The other four Mg II absorbers, at z_{abs} ~ 0.75-0.85, are stable with $\Delta N/\langle N \rangle$ in the range 6-20% at 1σ confidence level. Among them, the one in the spectrum of AO 0235+164 is 150 km s^{-1} away from the tentatively variable system.

In Bergeron et al. (2011), we found a potential excess of Mg II systems at $\beta \approx 0.1$ in blazar spectra and proposed that gas swept up by the AGN jet could be responsible for it. In such a scenario, absorption line variability can be expected, but, in the absence of predictions from numerical simulations, it is difficult to anticipate the time-scale and magnitude expected for the column density changes (this should strongly depends on the occurrence of marked variations in the activity of the nucleus itself at about the time when the blazar was observed). Thus, we cannot really draw conclusions from the lack of clear evidence for time variations among the limited set of systems which we could investigate here.

4.2. Structure in moderately ionized halo gas

We now discuss systems involving narrow absorption lines associated with halo gas which is optically thick to UV ionizing radiation, i.e. gas classically traced by Mg II or Fe II transitions. We mentioned above the few cases for which we could get stringent upper limits on column density variations for discrete velocity components seen through intermediate opacity lines. One good example is the z_{abs} = 1.3606 system toward FBQS J2340−0053 involving 10 Fe II components. Even when most of the absorption profile is optically thick (this is often the case for the Mg II doublet), the data can be used to search for variations near the profile edges (e.g. appearance or disappearance of faint components). We could not identify any change of this kind. Moreover, since the component redshifts are let free when fitting the profiles, we could also get constraints on velocity variations; again,
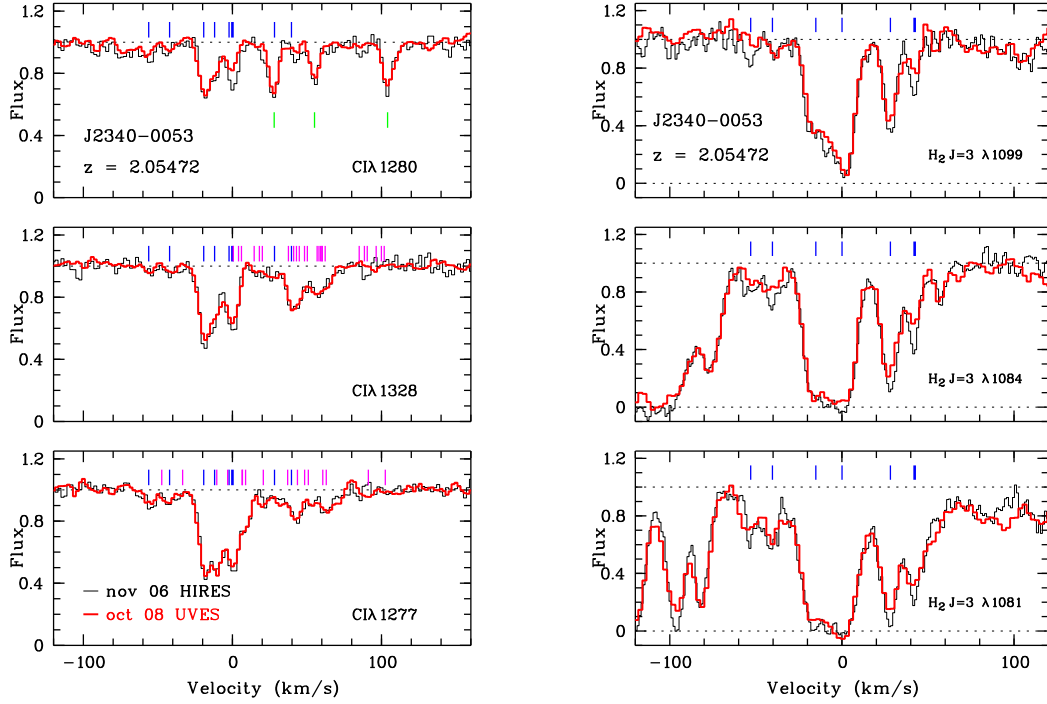
Fig. 3. C I λ1277, 1280, 1328 and molecular H_2, J=3 λ1081, 1084, 1081 absorptions at z_{abs} = 2.05472 toward FBQS J2340−0053 in the November 2006 (HIRES, black line) and October 2008 (UVES, red line) spectra. *Left panel*: the eight C I components required to fit the profiles are shown by blue tick marks and the marginally varying feature is at $v = 0$ (thick tick mark). In the top C Iλ1280 plot, three C Iλ1656 lines from the z_{abs} = 1.3606 system are also shown (green tick marks). For the C Iλ1277 and C Iλ1328 transitions, we show the position expected for C I* transitions associated with the 8 components (cyan tick marks); note that the features at $v \simeq$ 40 km s^{-1} are mainly due to C I* transitions. *Right panel*: six H_2 J=3 components are required to fit the profiles. Marginal variability is seen in the sixth component (thick tick mark) at $v \simeq$ 40 km s^{-1} (some difference is also seen in the fifth component but it is significant only at the 2.0σ level, instead of 3.1σ for the sixth one). For both narrow components displaying marginal variations in C I ($v \simeq$ 0) or H_2 ($v \simeq$ 40 km s^{-1}), we checked that the slightly higher resolution of the HIRES spectrum cannot account for the observed difference between the profiles.

we found no significant change, with 3σ upper limits generally below 1 km s^{-1}. Occasionally, some line profiles are observed to be rather smooth as seen for the resolved S IIλ1253 and 1259 lines at z_{abs} = 2.05454 in the FBQS J2340−0053 spectrum. As shown in Fig. 6, no significant difference is seen along the entire profile. The 1σ upper limit on the relative flux variation is 1.7 10^{-2} per resolution element along the S IIλ1259 line profile. Since the latter spans over 120 km s^{-1}, the previous upper limit applies to about 120/6.6 $\simeq$ 18 distinct resolution elements.

To conclude for these systems, we detected no structure in the density and velocity field within Mg II/Fe II halos at the scales that we could probe (typically of the order of 100 au). This is consistent with previous observations of moderately ionised gas in galaxy halos. Indeed, both Rauch et al. (2002) and Kobayashi et al. (2002) find that a typical value for the cloud size associated with the individual velocity components is 200 pc, implying very little structure at the much smaller scales that we probe here. We also note that, from the analysis of the number density of strong Mg II systems detected on top of quasar emission lines in SDSS spectra, Lawther et al (2012) derive a lower limit of about 0.03 pc for the individual Mg II absorbing clouds. Finally, Welty (2007) analysed multi-epoch HST spectra of HD 219188 and detect no variations for S II, O I, Si II and Fe II in the disk of our own Galaxy, over scales of the order of 100 au. Thus, our results are in good agreement with all known constraints on structure in moderately ionised gas.

In this context, the variations tentatively detected by Hacker et al. (2013) for narrow intervening Mg II systems are most surprising. These authors analysed more than 1000 reliable quasar absorption systems with multi-epoch observations and extracted a small subset of 33 systems displaying some evidence for time changes in their equivalent widths. Their study differs markedly from ours in the number of systems investigated and, given the small fraction of systems showing variability - about 3% - it is true that we expect very few variable lines in our sample. However, it should be stressed that the two studies differ also strongly in the sensitivity expressed in terms of ΔW_r or $\Delta W_r/W_r$. The variations reported in the SDSS spectra are very large with in most cases $\Delta W_r > 0.3$ Å and $\Delta W_r/W_r > 50\%$, corresponding to even larger fractional column density variations. For comparison, the marginal variation quoted above in the Mg IIλ2796 line at z_{abs} = 0.83032 toward PKS 1229−02 is smaller than $\Delta W_r = 0.01$ Å and $\Delta W_r/W_r = 5\%$.

If the large variations quoted by Hacker et al. (2013) are real, one can imagine that the number of systems expected to display changes at the level that we can reach in our high resolution study should be much larger, coming in contradiction with the absence of clear detection of variations in our sample. Before drawing any conclusion, additional observations aiming at confirming the status of the 33 potentially variable systems would be highly desirable. In particular, since variations are (to first or-
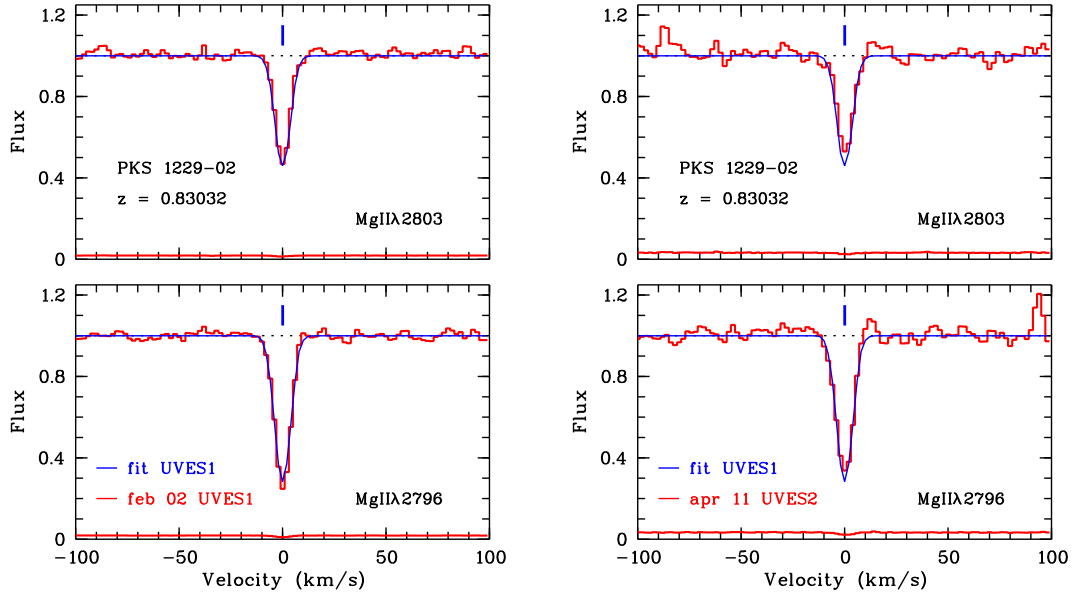
Fig. 5. Intervening Mg II absorption at $z_{abs} = 0.83032$ toward PKS 1229−02: spectrum and its error (red curves) together with simultaneous fit to both transitions (blue curve). In the left panel, we show the UVES 2002 data, while the right panel displays the UVES 2011 data with the fit performed on the UVES 2002 spectrum. The blue vertical tick mark underlines the marginally variable Mg II doublet.

Table 3. Targets with absorption systems showing marginal or significant variability.

target	z_{abs}^+	date	N cm^{-2}	date	N cm^{-2}
AO 0235+164	Mg II	(blend)	marginal variability[a]		
	0.85232	12-1997	$(2.79 \pm 0.46) \times 10^{12}$	02-2007	$(2.82 \pm 0.38) \times 10^{12}$
	0.85237[v]	12-1997	$(5.58 \pm 0.85) \times 10^{12}$	02-2007	$(3.25 \pm 0.57) \times 10^{12}$
	Mg II		no variability		
	0.85562	12-1997	$(7.27 \pm 0.36) \times 10^{11}$	02-2007	$(7.84 \pm 0.28) \times 10^{11}$
PKS 1229−02	Na I		significant variability[b]		
	-0.00013[v]	02-2002	$(1.98 \pm 0.41) \times 10^{11}$	04-2011	$(4.6 \pm 1.5) \times 10^{10}$
	-0.00010	02-2002	$(1.81 \pm 0.20) \times 10^{11}$	04-2011	$(1.67 \pm 0.16) \times 10^{11}$
	Mg II		no variability		
	0.76836	02-2002	$(7.15 \pm 0.24) \times 10^{11}$	04-2011	$(7.57 \pm 0.58) \times 10^{11}$
	Mg II		marginal variability[c]		
	0.83032[v]	02-2002	$(3.42 \pm 0.07) \times 10^{12}$	04-2011	$(2.87 \pm 0.13) \times 10^{12}$
FBQS J2340−0053	C I	(blend)	marginal variability[d]		
	2.05470	08-2006	$(1.33 \pm 0.16) \times 10^{13}$	10-2008	$(1.25 \pm 0.07) \times 10^{13}$
	2.05473[v]	08-2006	$(3.13 \pm 0.49) \times 10^{13}$	10-2008	$(1.52 \pm 0.23) \times 10^{13}$
	H$_2$,J=3		marginal variability[d]		
	2.05499	08-2006	$(1.66 \pm 0.10) \times 10^{15}$	10-2008	$(1.43 \pm 0.09) \times 10^{15}$
	2.05513[v]	08-2006	$(6.19 \pm 0.50) \times 10^{14}$	10-2008	$(4.39 \pm 0.31) \times 10^{14}$

[a,b,c,d] See Fig. 4, 2, 5, 3 (left panel), 3 (right panel).
[v] Significant variability: significance level $>3.5\sigma$ and $\Delta N/\langle N \rangle > 25\%$.
[v] Marginal variability: significance level either in the range 2.0-3.5σ or $>3.5\sigma$ but $\Delta N/\langle N \rangle < 25\%$.

der) expected to be regular, a third spectrum should confirm the trend observed on the two first ones. Such a work is currently in progress (see Appendix B2 in Dawson et al. 2013). Repeated *high resolution* observations of the brightest quasars involved would also be very useful to check the reality of time variations and to characterize them.

4.3. High z neutral/molecular gas

C I and H$_2$ are known to be closely related in diffuse molecular clouds (Srianand et al. 2005). Indeed, the velocity components found for both species are generally similar, although some significant differences in their relative strength can be observed, as is the case for the $z_{abs} = 2.0545$ system toward
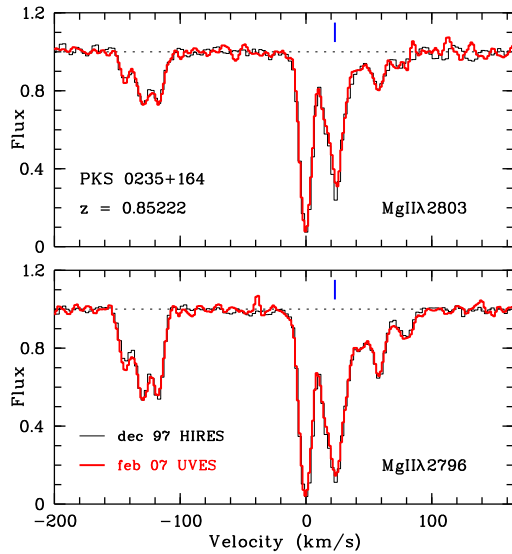
Fig. 4. Intervening Mg ɪɪ absorption at z_{abs} = 0.852 toward AO 0235+164 in the December 1997 (HIRES, black line) and February 2007 (UVES, red line) spectra (lower panel: Mg ɪɪλ2796; upper panel: Mg ɪɪλ2803). The blue vertical tick mark underlines a marginally variable blended component at z_{abs} = 0.85237, although at a 2.3σ significance level only.

FBQS J2340−0053 (Sect. 3.3 and Fig 3). We successively discuss these two tracers below.

C ɪ lines are detected in three high z systems, one toward PKS 0458−020 and two toward FBQS J2340−0053, but useful constraints could be obtained only for the latter two at z_{abs} = 1.3606 (no change in N) and 2.0454 (possible variation of about 70% for an unresolved component). Unfortunately, since i) the transverse velocity of the quasar is unknown and ii) the LoS drift is determined solely by the quasar motion for the z_{abs} = 2.0545 system because $z_{abs} \simeq z_{em}$, it is not possible to compute the scale probed through the neutral gas. Further, the transverse observer's velocity for this target being only 12 km s^{-1}, little drift due to the observer's motion is expected for the z_{abs} = 1.3606 absorber. We can then just get a typical value for the drifts by assuming a transverse velocity of about 300 km s^{-1} for the intervening galaxies. This value together with a time interval of 1.9 yrs (observer's frame) between the two observations corresponds to a linear scale of about 50 and 40 au at z_{abs} = 1.3606 and 2.0545 respectively. In our own Galaxy, the available information on structure in the C ɪ distribution remains quite limited. Welty (2007) performed a detailed study of the time behavior observed for visible and UV transitions due to an intermediate velocity cloud toward the star HD 219188. Variations by a factor of about two are seen for Na ɪ, C ɪ and Ca ɪɪ column densities over scales of tens of au. Qualitatively, Na ɪ and C ɪ display the same time behavior, indicating that the more extensive results obtained on the Na ɪ structure (Crawford, 2003; Smoker et al. 2011) are probably valid also for C ɪ. In this context, results obtained for N(C ɪ) at z_{abs} = 1.3606 and 2.0545 are certainly consistent with

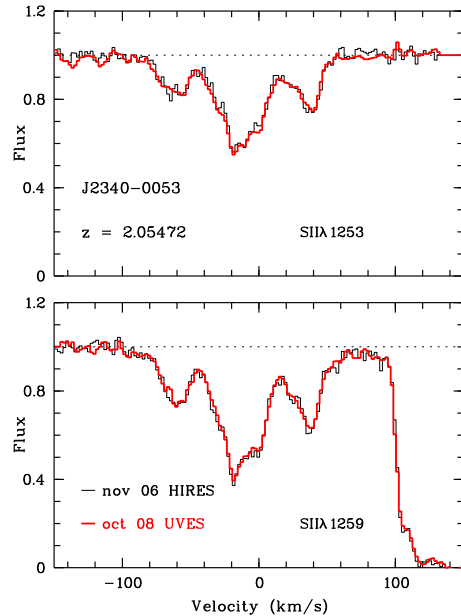**Fig. 6.** S ɪɪ$\lambda\lambda$1253, 1259 absorption at z_{abs} = 2.05454 toward FBQS J2340−0053 in the november 2006 (HIRES, black line) and october 2008 (UVES, red line) spectra.

the properties known for Galactic gas. Clearly, studies involving more systems are desirable to reach firm conclusions.

Regarding H$_2$, velocity components number 5 and 6 display an intermediate opacity which provides a good sensitivity for the $J = 3$ column densities (the other $J = 3$ components are either too weak or too saturated; similarly, $J = 2$ lines are too strong while $J = 4$ are too weak to be suitable). The detection of marginal variations in component number 6 is interesting in the context of questions related to the "warm H$_2$" observed along many Galactic LoS (Gry et al. 2002; Jensen et al. 2010). UV pumping is generally found to be insufficient to explain the observed excess of $J \geq 2$ H$_2$ with respect to the amount expected for a thermal distribution (Gry et al. 2002). Small structures (like shocks or turbulent vortices) where the temperature can locally reach high values have been proposed to account for both the production of species like CH$^+$ and the relative amount of $J \geq 2$ H$_2$ (Godard et al. 2009). Presently, there are no direct constraints on the size of these putative regions. In our Galaxy, the only repeated measurements in the far-UV were performed toward the runaway O star, HD 34078 (Boissé et al. 2009). Stringent constraints were derived from the analysis of damped line profiles associated with $J = 0$ lines, but no limit could be obtained for the $J = 2, 3, 4$ levels because the corresponding lines are insensitive to small relative changes in N. It is noticeable that for the varying component toward FBQS J2340−0053, the $N(J = 0, 1, 2, 3)$ values (1.39 $\times 10^{17}$, 2.61 $\times 10^{17}$, 4.71 $\times 10^{15}$ and 5.28 $\times 10^{14}$ cm^{-2}; for the $J = 3$ column density, we give the average of the 2006 and 2008 values) are consistent with a unique excitation temperature, T_{ex} = 120 K, unlike what is seen over most of Galactic LoS where an excitation temperature of about 300 K is required to fit $N(J)$ values at $J \geq 2$ (Jensen et al. 2010). This indicates that the gas is dense enough to ensure thermalisation, in qualitative agreement with the small size suggested by the presence of time variations for this component.

4.4. Local Galactic gas

We found a large variation (factor of four) in Galatic $N(\text{Na I})$ for one of the five velocity components toward PKS 1229−02. The constraint on the corresponding cloudlet size can be estimated from the peculiar motion of the Sun with respect to the LSR (see Sect. 2.2). For this direction, the Sun's velocity is mostly transverse with V_t (Sun)/LSR = 17.8 km s^{-1}, implying a drift of about 35 au (this is only an estimate since we cannot know the transverse velocity of the cloud). This is well within the range (typically a few 10 au or larger) for which Na I line changes have been observed on other LoS (Crawford 2003). The other four components toward PKS 1229−02 remained stable over the same linear scale, indicating that the associated fragments are characterised by sizes larger than 100 au. For other targets providing useful constraints on Galactic gas structure, we find variation neither toward AO 0235+164 nor toward FBQS J2340−0053. The transverse velocity of the Sun for these two targets is 15.8 km s^{-1} and 16.6 km s^{-1} respectively, implying drifts of about 30 and 7 au in local material. In these two cases, Na I lines have a relatively large opacity implying a poor sensitivity to variations.

Toward PKS 1741−038, the estimated drift over the 9.8 yr separating the two observations is about 17 au. The absence of variations in DIBs near 5780.5 and 5797.1 Å can be related to results obtained recently by Cordiner et al. (2013) for ρ Oph stars. These authors find variations of about 5-9% for the above DIBs over scales exceeding 300 au. Thus, given our limited sensitivity, the observed stability is not surprising.

5. Summary and prospects for further studies

As discussed above, the only clear and unambiguous variation has been detected for the Na I doublet from our own Galaxy toward PKS 1229−02, in good agreement with previous results on the au-scale structure of neutral Galactic gas. In the same kind of media but at higher redshifts ($z \approx 2$ toward FBQS J2340−0053), we also find tentative evidence for structure in neutral and molecular gas : C I with $\Delta N/\langle N\rangle \simeq 70\%$ at the 3.0σ significance level and H$_2$ with $\Delta N/\langle N\rangle \simeq 35\%$, at the 3.1σ level. For low β absorption systems in blazar spectra, absorption profiles are, for the most part, very stable and only a marginal 3.7σ 17% variation has been seen in the strength of a narrow Mg II component toward PKS 1229−02. On the other hand, no change was seen for moderately ionised gas at high β (i.e. intervening halo gas), which again is consistent with known constraints on typical cloud sizes in such media.

The results discussed above illustrate well the potential and the limits of the method used in this paper to investigate the small-scale structure of absorbing gas in quasar spectra. Let us first outline the great value of high spectral resolution. Often, several transitions from the same species are detected and can be used to fit absorption line profiles, thus yielding well constrained b and N values for the velocity components seen at each epoch. This redundancy provides a powerful objective way (at least for those components which are partially resolved) to assess the reality of time changes and rule out false variations. Indeed, it is very unlikely to find by chance two artefacts mimicking true variations, i.e. occurring on two line profiles at the same position in velocity space and with a strength consistent with the f values of the transitions involved. If species displaying more than two transitions (like C I or H$_2$) can be used to increase the redundancy and the range covered by f values, the probability is even lower and better constraints can be derived from line fitting. Conversely, the Mg II system at $z_{abs} = 0.85236$

toward AO 0235+164 illustrates well that with only two transitions differing in their f values by a factor no larger than two, one may be unable to reach firm conclusions when variations are moderate. Furthermore, high resolution allows us to quantify the changes in meaningful astrophysical parameters, N and b values, or to set upper bounds on their variations. Limitations appear however for some line profiles (e.g. the C I component toward FBQS J2340−0053 for which variations are suspected), when the decomposition into discrete components required by line fitting is poorly defined or not unique. Such difficulties mean that the spectral resolution used is not high enough to analyse properly the velocity distribution, implying that line opacities as well as N and b values cannot be determined reliably. One should therefore prefer absorption systems with simple velocity structure for repeated observations.

In our study, we considered several topics for which useful constraints can be obtained from an investigation of time variations. We now discuss prospects for two of them. We mentioned above that generally, we have a poor knowledge of the scales probed by repeat observations because the transverse motion of the target is not measurable. The situation is more favorable for low redshift absorbers because the drift of the LoS through the intervening gas is determined mainly by the observer's motion, which is inferred directly from observations of the CMB dipole. For instance, in order to study whether the small-scale structure seen in the Galactic neutral or weakly ionised gas is ubiquitous in external galaxies, one could reobserve quasars belonging to the so-called quasar-galaxy pairs (see e.g. Bowen et al. 1991) and search for temporal changes in the Ca II or Na I lines over more than 20 years. Of course, targets located in directions which are more or less normal to our large-scale peculiar velocity should be preferred (in this favorable configuration, the scales probed over 20 years are of the order of 1500 au). Regarding high redshift absorbers, for which only a rough estimate of the scales probed can be obtained, one needs to observe a statistically significant sample of targets to derive meaningful results concerning the presence and strength of small-scale structure. Some quasars are found in pairs (Hennawi et al. 2010) and occasionally, absorbers appear to belong to galaxy clusters (Whiting et al. 2006) implying increased peculiar velocities. Such LoS will, in average, be associated with larger drifts, and should be targetted preferentially.

A second topic for which repeated observations of quasars at high spectral resolution are especially timely involves the properties and origin of the warm ($J \geq 2$) H$_2$ found in diffuse molecular gas in our own Galaxy, as well as in high redshift absorbers. During the past ten years, the number of high z H$_2$ systems has increased very significantly and now exceeds 20 (Albornoz-Vásquez et al. 2014). Some of them display narrow velocity components which are well suited to a detailed study (see e.g. Noterdaeme et al. 2007). As discussed in Sect. 3 for the system at $z_{abs} = 2.0545$ toward FBQS J2340−0053, multi-epoch observations can provide key information on the typical size of regions where diffuse molecular gas is heated to temperatures above 200 K. Such high z warm H$_2$ is seen at epochs when star formation was much larger than today (Madau & Dickinson 2014) and one can therefore anticipate that the diffuse molecular medium should be strongly impacted by a very high dissipation rate of the mechanical energy carried by shock waves and turbulence.

To conclude, we wish to stress that the data used here were acquired for purposes other than variability searches and thus, are certainly not optimal for our study. First, the two spectra available for each target often differ significantly in their S/N

ratio and one is then limited in the comparison by the lower quality spectrum. The time interval also varies a lot from target to target (unfortunately, the lag for the quasar displaying the richest spectrum - FBQS J2340−0053 - is of only two years). A straightforward strategy to get better constraints or address some questions discussed above with more appropriate data would consist in i) selecting targets displaying the required types of absorption lines and with one already available good high resolution spectrum taken at least 10 years ago, and ii) reobserving them at a similar S/N and resolution. Obviously, the existence of databases where high resolution quasar spectra are archived properly are extremely useful in such an approach. Finally, we note that improvements in the accuracy of wavelength calibrations accomplished recently in the context of the ESO Large Program designed to constrain the variation of fundamental constants (Molaro et al. 2013) or forseen for instruments that will become available in the near future (e.g. the *ESPRESSO* spectrograph to be mounted on the ESO/VLT telescope) should indeed help to investigate in more detail the velocity field within the absorbers.

References

Akeson, R.L. & Blitz, L. 1999, ApJ, 523, 163

Albornoz-Vàsquez, D., Rahmani, H., Noterdaeme, P. et al. 2014, A&A, 562, 88

Bergeron, J., Boissé, P. & Ménard 2011, A&A, 525, A51

Bergeron, J., Petitjean, P., Aracil, B. et al. 2004, The Messenger, 118, 40

Boissé, P., Rollinde, E., Hily-Blant, P. et al. 2009, A&A, 501, 221

Boissé, P., Federman, S. R., Pineau Des Forêts, G. & Ritchey, A. M. 2013, A&A, 559, A131

Bowen, D. V., Pettini, M., Penston, M. V. & Blades, C. 1991, MNRAS, 249, 145

Burbidge, E. M., Beaver, E. A., Cohen, R. D., Junkkarinen, V. T. & Lyons, R. W. 1996, AJ, 112, 2533

Chen, Z.-F., Pan, C.-J., Li, G.-Q., Huang, W.-R. & Li, M.-S. 2013, JApA, 34, 317

Churchill, C. W. & Charlton, J. C. 1999, AJ, 118,59

Cordiner, M. A., Fossey, S. J., Smith, A. M. & Sarre, P. J. 2013, ApJ, 764, 10

Crawford, I. A. 2003, Ap&SS, 285, 661

Crighton, N. H. M., Hennawi, J. F., Simcoe, R. A. et al. 2015, MNRAS, 446, 18

Dai, X., Kochanek, C. S., Chartas, G. et al. 2010, ApJ, 709, 278

Dawson, K. S., Schlegel, D. J., Ahn, C. P. et al. 2013, AJ, 145, 10

Filiz Ak, N., Brandt, W. N., Hall, P. B. et al. 2013, MNRAS, 777, 168

Fixsen, D. J., Cheng, E. S., Gales, J. M. et al. 1996, ApJ, 473, 576

Godard, B., Falgarone, E. & Pineau Des Forêts, G. 2009, A&A, 495, 847

Grier, C. J., Hall, P. B., Brandt, W. N. et al. 2015, ArXiv 1503.030706

Gry, C., Boulanger, F., Nehmé, C. et al. 2002, A&A, 391, 675

Hacker, T. L., Brunner, R. J., Lundgren, B. F. & York, D. G. 2013, MNRAS, 434, 183

Heiles, C. & Steinebring, D. 2007, ASPC, 365, 331

Hennawi, J. F., Myers, A. D., Shen, Y. et al. 2010, ApJ, 719, 1672

Hamann, F., Kaplan, K. F., Rodriguez Hidalgo, P., Prochaska, J. X. & Herbert-Fort, S. 2008, MNRAS, 391, L39

Hamann, F., Kanekar, N., Prochaska, J. X. et al. 2011, MNRAS, 410, 1957

Jensen, A. G., Snow, T. P., Sonneborn, G. & Rachford, B. L. 2010, ApJ, 711, 1236

Jorgenson, R. A., Wolfe, A. M. & Prochaska, J. X. 2010 ApJ, 723, 460

Kanekar, N. & Chengalur, J. N. 2001, MNRAS, 325, 631

Kanekar, N., Prochaska, J. X., Ellison, S. L. & Chengalur, J. N. 2010 ApJ, 712, L152

Kanekar, N., Prochaska, J. X., Smette, A. et al. 2014, MNRAS, 438, 2131

Kobayashi, N., Terada, H., Goto, M. & Tokunaga, A. 2002, ApJ, 569, 676

Lauroesch, J. T. 2007, ASPC, 365, 40

Lawther, D., Paarup, T., Schmidt, M. et al. 2012, A&A, 546, A67

Lazio, T. J. W., Gaume, R. A., Claussen, M. J. et al. 2001, ApJ,546, 267

Le Brun, V., Bergeron, J., Boissé, P. & Deharveng, J. M. 1997, A&A, 321, 733

Levshakov, S. A., Dessauges-Zavadsky, M., D'Odorico, S. & Molaro, P. 2002, ApJ, 565, 696

Lucas, R. & Liszt, H. 1996, A&A, 307, 252

Lucas, R. & Liszt, H. 2000, A&A, 358, 1069

Madau, P. & Dickinson, M. 2014, ARA&A, 52, 415

Meyer, D. M., Peek, J. E. G., Peek, J. E. G. & Heiles, C. 2012, ApJ, 752, 119

Misawa, T., Charlton, J. C. & Eracleous, M. 2014, ApJ, 792, 77

Molaro, P., Centurión, M., Whitmore, J. B. et al. 2013, A&A, 555, A68

Narayanan, D., Hamann, F., Barlow, T. et al. 2004, ApJ, 601, 715

Neeleman, M., Prochaska, J. X. & Wolfe, A. M. 2015, ApJ, 800, 7

Noterdaeme, P., Ledoux, C., Petitjean, P. et al. 2007, A&A, 474, 393

Rahmani, H., Srianand, R., Gupta, N. et al. 2012, MNRAS, 425, 556

Rauch, M., Sargent, W. L. W., Barlow, T. A. & Simcoe, R. A. 2002, ApJ, 576, 45

Savage, B. D. & Sembach, K. R. 1991, ApJ, 379, 245

Srianand, R., Petitjean, P., Ledoux, C., Ferland, G. & Shaw, G. 2005, MNRAS, 362, 549

Smoker, J. V., Bagnulo, S., Cabanac, R. et al. 2011, MNRAS, 414, 59

Takalo, L.O., Sillanpaeae, A., Valtaoja, E. et al. 1998, A&AS, 128, 577

Welty, D. E. 2007, ApJ, 668, 1012

Whiting, M. T., Webster, R. L. & Francis, P. J. 2006, MNRAS, 368, 341

Wise, J. H., Eracleous, M., Charlton, J. C. & Ganguly, R. 2004, ApJ, 613, 129

Wolfe, A. M., Davis, M. M. & Briggs, F. H. 1982, ApJ, 259, 495